Egyptian Journal of Physics
https://ejphysics.journals.ekb.eg/

Dependence of refractive index of Zamzam, bottled drinking, and distilled waters on temperature and wavelength: a simple approximation using computer simulation phase shifting digital interferometry

Nasser A. Moustafa

Helwan University, Faculty of Science, Physics department, Cairo, Egypt.

Abstract

In this study, the variations in refractive indices of Zamzam, bottled drinking, and distilled waters with wavelengths and temperatures in the range of 20°C to 80°C have been measured by computer simulation phase shifting digital interferometry at six discrete wavelengths across the visible spectrum. The computer simulation phase shifting digital interferometer have been used to design an experimental setup to investigate the wrapped images of the correlation fringes. By having the derivatives of the refractive index of the liquid with respect to the temperature T, $\left(\frac{dn_\ell}{dT}\right)$ and the wavelength, λ, $\left(\frac{dn_\ell}{d\lambda}\right)$ respectively from the new equation of refractive index, the dependence on temperature and wavelength was obtained. In this paper, a new theoretical model about the temperature dependence of the refractive index of liquid is presented, and it is in agreement with the previous experimental results. In summary, bottled drinking and distilled waters do not have the unique and distinctive optical refractive index that Zamzam water does.

Keywords: speckle photography, phase-shifting digital interferometry, water refractive index, wavelength dependence, temperature dependence.

1. Introduction

The index of refraction is a fundamental optical property of materials, and its accurate value is often required in many branches of physics and chemistry. It also has several applications in many industries and materials to determine the purity of glass and hard plastic materials [1–4]. By measuring the refractive index of the binary

*Corresponding author: Nasser A. Moustafa, E-mail: nasseramoustafa@gmail.com.
Received: 08/01/2024; Accepted: 26/01/2024
DOI: 10.21608/EJPHYSICS.2024.261329.1098

solution, the composition of the solution can be determined [3, 4]. Therefore, refractive index measurements are widely used in many industrial and research applications to determine a solution's concentration [5, 6]. There is a variation of the refractive index with concentration, temperature, pressure, and wavelength [2–6]. Recent studies [2-4] provided a detailed study on concentration mapping by measuring the refractive index of liquid. The temperature coefficient of refractive index can also be used to calculate the thermal expansion coefficient [2, 4]. Several techniques have been reported in the literature to measure the concentration and temperature dependence of the refractive index of a sugar solution [2–7]. Jenkins [8] proposed a method using a laser for the measurement of variations in the refractive indices due to the change in concentration of a solution. Rahman [9] studied the variations of refractive index using the method of Bass and Weidner [10] for the case when the concentration of a solution is altered from distilled water to a saturated condition. They measured the refractive indices of liquid solutions at the He-Ne laser wavelength using the conventional minimum deviation method of an equilateral hollow glass prism. This method was identical to that described by Jenkins [8], except that instead of a screen, a telescope was used to find the minimum angle of deviation.

Therefore, the goal of this study is to extend the applicability of the computer simulation phase shifting digital interferometry [11] to measure the dependence of the refractive index of Zamzam, bottled drinking, and distilled waters on the variation of temperature and wavelength. An empirical expression was also derived for given the relation between the change in the temperature of the liquid and the separation between a pair of identical speckle pattern $\Delta\xi$, which clarifies the calibration process of the illustrated computer simulation set-up.

2. Theoretical background

For measuring the change in refractive index of a liquid, it is placed between two thin glass slides, as shown in Fig. 1, which is an illustration of a computer simulation to monitor the correlation fringes in the spectral field for Zamzam, bottled,bottled and distilled waters. Spatially coherent light travels through a system of two glass slides and the liquid between them, illuminating a rough surface.

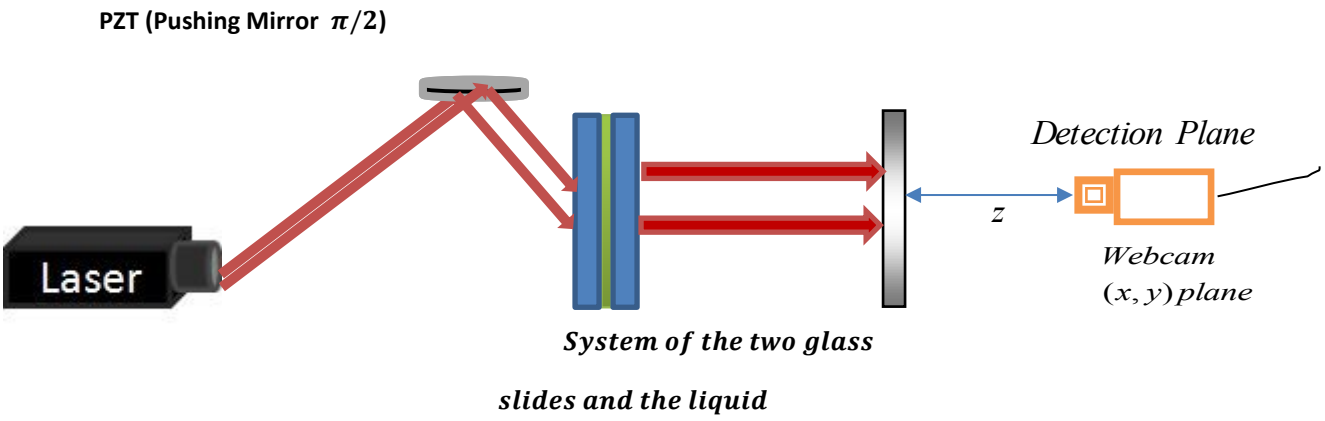

Fig. 1. Illustration of computer simulation for observation of correlation fringes and phase map in the spectral field for Zamzam ,bottled drinking and distilled waters.

By applying rotation and non-rotation states to the incident laser beam and by falling the transmitted beam on the rough surface, as a result, there are two images on the observation plane (CDD plane), which are digitally combined [12] to give the correlation fringes.

$$A_1(x,y)=\frac{1}{j\lambda z}ae^{i\phi}e^{jkz}e^{-i(k_1d_1+k_2d_2+k_3d_3)}e^{\frac{j\pi}{\lambda z}(x^2+y^2)}F\{A(\xi,\eta)\} \tag{1}$$

If the incident plane wave makes an angle with the x-axis of the system and is transmitted through the two glass slides and the liquid, The incident plane wave continues to propagate as a plane wave with wavenumber k. The amplitude distribution $A_2(x,y)$ after the second exposure, which can be obtained with an angle of incidence θ of the plane wave and observed in the observation plane and is given as:

$$A_2(x,y)=\frac{1}{j\lambda z}ae^{i\phi}e^{jkz}\exp-jk_1(d_1).\exp-jk_1d_1\left(\frac{\theta^2}{2n_g^2}\right).\exp-jk_2(d_2).\exp-jk_2d_2\left(\frac{1}{2}.\frac{\theta^2}{n_g^2n_\ell^2}\right).\exp-jk_3(d_3).$$
$$\exp-jk_3d_3\left(\frac{1}{2}\frac{\theta^2}{n_\ell^2n_g^4}\right)e^{\frac{j\pi}{\lambda z}(x^2+y^2)}.\exp(j2\pi\Delta\xi\omega_x)F\{A(\xi,\eta)\} \tag{2}$$

$$A_2(x,y)=\frac{1}{j\lambda z}ae^{i\phi}e^{jkz}\exp-jk_1(d_1).\left(1+\frac{\theta^2}{2n_g^2}\right).\exp-jk_2(d_2).\left(1+\frac{1}{2}.\frac{\theta^2}{n_g^2n_\ell^2}\right).\exp-jk_3(d_3).\left(1+\frac{1}{2}\frac{\theta^2}{n_\ell^2n_g^4}\right)$$
$$.e^{\frac{j\pi}{\lambda z}\left(x^2+y^2\right)}.\exp\left(j2\pi\Delta\xi\omega_x\right)F\{A(\xi,\eta)\} \tag{3}$$

By adding the two equations (1) and (3), the intensity distribution in the observation plane can be written as,

$$I=\left(\frac{1}{\lambda z}\right)^2F^2\{A(\xi,\eta)\}.\left(2+2\cos\left(2\pi\Delta\xi\omega_x-kd_1\frac{\theta^2}{2n_g^2}-kd_2\frac{\theta^2}{2n_g^2n_\ell^2}-kd_3\frac{\theta^2}{2n_\ell^2n_g^4}\right)\right) \tag{4}$$

At maximum intensity, and where m=1,

$$2\pi\Delta\xi\omega_x-kd_1\frac{\theta^2}{2n_g^2}-kd_2\frac{\theta^2}{2n_g^2n_\ell^2}-kd_3\frac{\theta^2}{2n_\ell^2n_g^4}=2m\pi \tag{5}$$

From equation (5), an equation for the refractive index of a liquid can be obtained [13].

The refractive index is given by:

$$n_\ell=\sqrt{\frac{\left(\frac{d_2}{\lambda}\frac{\theta^2}{2n_g^2}+\frac{d_3}{\lambda}\frac{\theta^2}{2n_g}\right)}{\left(\Delta\xi\omega_x-\frac{d_1}{\lambda}\left(\frac{\theta^2}{2n_g^2}-1\right)\right)}} \tag{6}$$

Where the thicknesses of the two glass slides are d_1 and d_3 respectively, also the thickness of the liquid is d_2. The incident plane wave continuous to propagate as a plane wave with wavenumbers k_1, k_2, and k_3 respectively. n_g is the refractive index of the glass plate.

Where $\omega_x=2\pi/\lambda_x$, and $\Delta\xi=M\xi_m=\lambda z/\lambda_x$, M is the magnification of the imaging system, and ξ_m is the mechanical displacement used for the calibration of the system [13-15].

The calibration process of the illustrated computer simulation set-up is made by measuring the values of $\Delta\xi$ with the corresponding values of the temperature. Figure (2) shows the calibration curve for given the relation between the change in the temperature of the liquid and the separation between a pair of identical speckle patterns $\Delta\xi$.

The obtained calibration equation is given by:

$$\Delta\xi = y_0 + A \times \exp(R_0 T) \tag{7}$$

y_0, A, and R_0 which are shown in the equation of the calibration of are considered as constants depending on the calibration process, and T is the applied temperature.

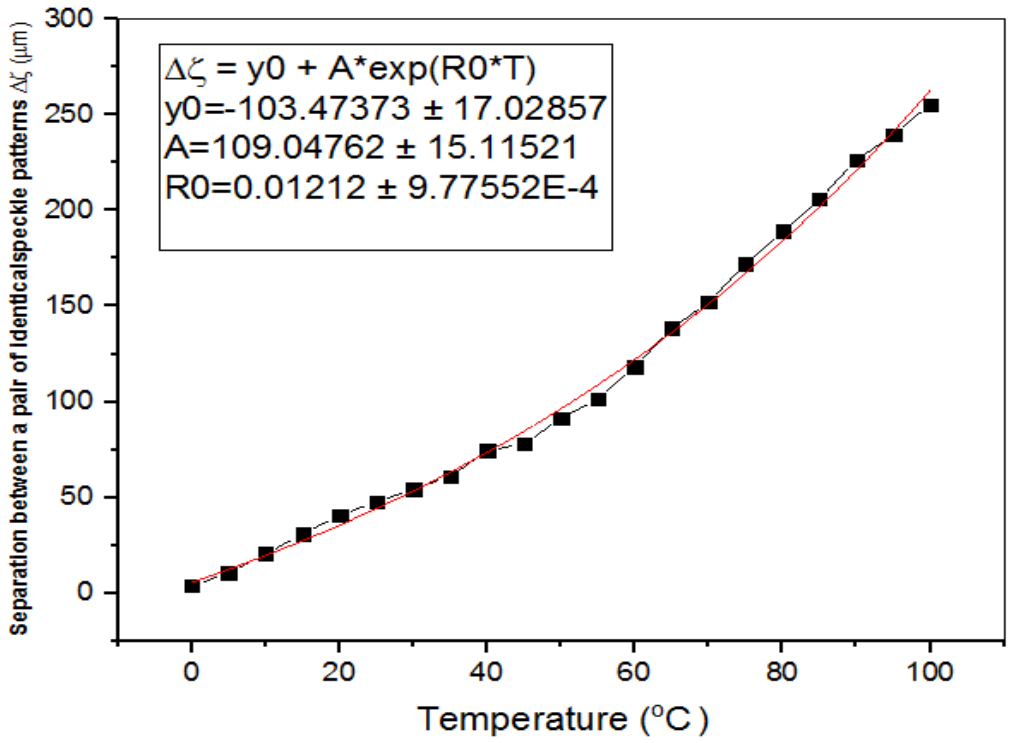

Fig. 2. The calibration curve for given the relation between the change in the temperature of the liquid and the separation between a pair of identical speckle pattern Δξ.

Equation (6) can be written as:

$$n_\ell = \sqrt{\frac{\left(\frac{d_2}{\lambda}\frac{\theta^2}{2n_g^2}+\frac{d_3}{\lambda}\frac{\theta^2}{2n_g}\right)}{\left(\omega_x\left(y_0+A\times\exp\left(R_0T\right)\right)-\frac{d_1}{\lambda}\left(\frac{\theta^2}{2n_g^2}-1\right)\right)}} \tag{8}$$

$$\frac{dn_\ell}{dT} = \frac{\left(\frac{d_2}{\lambda}\frac{\theta^2}{2n_g^2}+\frac{d_3}{\lambda}\frac{\theta^2}{2n_g}\right)^{1/2}\times\omega_x AR_0\exp\left(R_0T\right)}{\left(\omega_x\left(y_0+A\times\exp\left(R_0T\right)\right)-\frac{d_1}{\lambda}\left(\frac{\theta^2}{2n_g^2}-1\right)\right)^{3/2}} \tag{9}$$

Where $\frac{dn_\ell}{dT}$ represents the change in refractive with temperature.

$$\partial n_\ell/\partial\lambda = \left(\frac{-1}{2}\right)\frac{\left[\theta^2\left(d_2+d_3/n_g^2\right)/2n_g^2\right]^{1/2}\left(4\pi\frac{\Delta\xi}{\lambda_x}-1\right)}{\left[2\pi\frac{\Delta\xi}{\lambda_x}-\frac{d_1\theta^2}{2n_g^2}-\lambda\right]^{3/2}} \tag{10}$$

Equation (10) can be written as:

$$\partial n_\ell/\partial\lambda = \left(\frac{-1}{2}\right)\frac{\left[\theta^2\left(d_2+d_3/n_g^2\right)/2n_g^2\right]^{1/2}\left(\frac{4\pi}{\lambda_x}\left(y_0+A\times\exp\left(R_0T\right)\right)-1\right)}{\left[\frac{2\pi}{\lambda_x}\left(y_0+A\times\exp\left(R_0T\right)\right)-\frac{d_1\theta^2}{2n_g^2}-\lambda\right]^{3/2}} \tag{11}$$

Where $\partial n_\ell/\partial\lambda$ represents the change in refractive with wavelength.

For the phase measurement, which is required for the measurement of the refractive index of the waters, and consequently the change in the refractive index, five phase stepping algorithms were applied [16]. The phase shift

needed for automatic fringe analysis can be introduced by a piezoelectric transducer (PZT). The five-phase step algorithms was used with a phase shift $\pi/2$ per exposure. The intensity distribution of the corresponding correlograms can be expressed as [17].

$$I_1 = \left(\frac{1}{\lambda z}\right)^2 F^2\{A(\xi,\eta)\}\left(2 + 2\cos\left(2\pi\Delta\xi\omega_x - kd_1\frac{\theta^2}{2n_g^2} - kd_2\frac{\theta^2}{2n_g^2 n_\ell^2} - kd_3\frac{\theta^2}{2n_\ell^2 n_g^4} + \alpha_1\right)\right)$$

for $\alpha_1 = 0$ (12)

$$I_2 = \left(\frac{1}{\lambda z}\right)^2 F^2\{A(\xi,\eta)\}\left(2 + 2\cos\left(2\pi\Delta\xi\omega_x - kd_1\frac{\theta^2}{2n_g^2} - kd_2\frac{\theta^2}{2n_g^2 n_\ell^2} - kd_3\frac{\theta^2}{2n_\ell^2 n_g^4} + \alpha_2\right)\right)$$

for $\alpha_2 = \pi/2$ (13)

$$I_3 = \left(\frac{1}{\lambda z}\right)^2 F^2\{A(\xi,\eta)\}\left(2 + 2\cos\left(2\pi\Delta\xi\omega_x - kd_1\frac{\theta^2}{2n_g^2} - kd_2\frac{\theta^2}{2n_g^2 n_\ell^2} - kd_3\frac{\theta^2}{2n_\ell^2 n_g^4} + \alpha_3\right)\right) \quad (14)$$

for $\alpha_3 = \pi$

$$I_4 = \left(\frac{1}{\lambda z}\right)^2 F^2\{A(\xi,\eta)\}\left(2 + 2\cos\left(2\pi\Delta\xi\omega_x - kd_1\frac{\theta^2}{2n_g^2} - kd_2\frac{\theta^2}{2n_g^2 n_\ell^2} - kd_3\frac{\theta^2}{2n_\ell^2 n_g^4} + \alpha_4\right)\right) \quad (15)$$

for $\alpha_4 = 3\pi/2$

$$I_5 = \left(\frac{1}{\lambda z}\right)^2 F^2\{A(\xi,\eta)\}\left(2 + 2\cos\left(2\pi\Delta\xi\omega_x - kd_1\frac{\theta^2}{2n_g^2} - kd_2\frac{\theta^2}{2n_g^2 n_\ell^2} - kd_3\frac{\theta^2}{2n_\ell^2 n_g^4} + \alpha_5\right)\right) \quad (16)$$

for $\alpha_5 = 2\pi$

The phase needed for the measurement of the refractive index n_ℓ and the change in refractive index is obtained from the intensity distributions of Eqs. (12) to (16) and is given by:

$$\Phi = \tan^{-1}\frac{2(I_2 - I_4)}{2I_3 - I_5 - I_2} \quad (17)$$

The new equation of the refractive index n_ℓ is related to the fringe spacing λ_x, which can be determined accurately from the phase map of equation (16), mathematically from equation (8), and given by:

$$\lambda_x = \sqrt{\frac{2\pi\lambda z}{\frac{\theta^2\left(d_2 + d_3/n_g^2\right)}{2\lambda n_g^2 n_\ell^2} + \frac{d_1}{\lambda}\frac{\theta^2}{2n_g^2} + 1}} \tag{18}$$

Java-based image processing program was used for the calculation of the fringe spacing of the computer simulation results for given the refractive index.

3. Computer Simulation Results and Discussions

The illustration of the optical configuration, which is shown in Fig. 1, is implemented to present a comparative study of Zamzam , bottled drinking, and distilled waters by a computer simulation speckle photography method using Fourier transform. A coherent laser beam with six discrete wavelengths across the visible spectrum (λ =632.8 nm, 589.3 nm, 577.0 nm, 546.1 nm, 435.8 nm, and 404.7 nm, respectively) illuminates the system of the two glass slides and the liquid. The thicknesses of the two glass slides are $d_1 = 300\mu m$ and $d_3 = 300\mu m$ respectively, also the thickness of the liquid is $d_2 = 215\mu m$. As shown in Fig. 1, the laser beam spot at the diffuser plane was kept at 2 cm in diameter, and the distance between the rough surface and the imaging plane was Z = 75 cm.

The incident laser beam is exposed to two angles of incidence resulting from rotation and non-rotation processes, and consequently, two images on the observation plane (CDD plane) are obtained, which are combined digitally to give the correlation fringes. The rotation angle of the incident laser beam was $\theta = 0.2^\circ$.

The following figures 3 (a,b,c,d), 4 (a,b,c,d), and 5 (a,b,c,d) show the wrapped images of the correlation fringes in the spectral field at wavelength 0.6328 μm for Zamzam, bottled drinking, and distilled waters at different temperatures $20^\circ C$, $64^\circ C$, $76^\circ C$, and $80^\circ C$, respectively.

As we can see from these figures, for the same type of water, Zamzam, bottled drinking, or distilled waters, the wrapped image width increases with increasing temperature. Also, we can see that for the different types of

water, the wrapped image width at wavelength 0.6328 μm increases gradually with increasing temperature and decreasing the refractive index of the liquid. It means the largest width in the case of distilled water, which has the lowest refractive index.

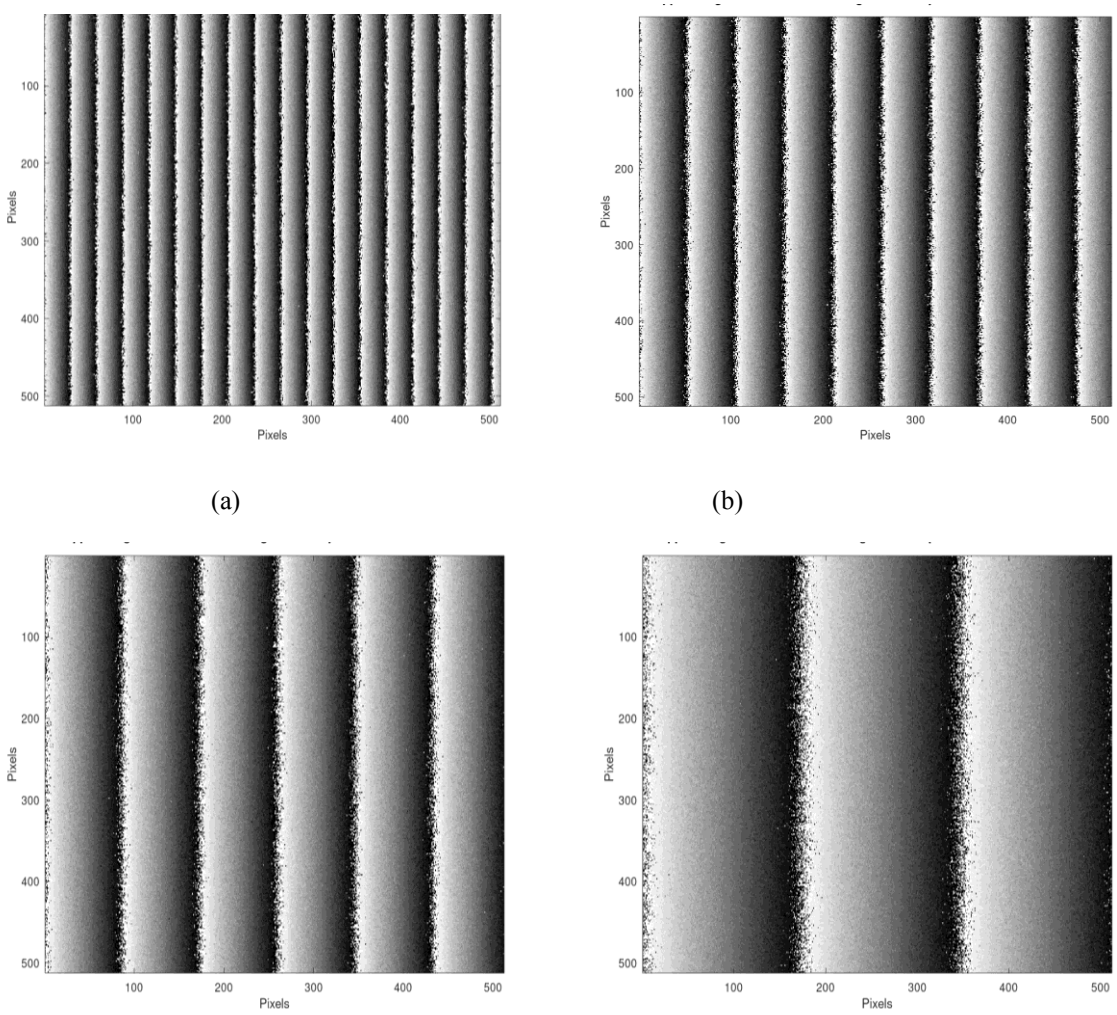

(a) (b)

(c) (d)

Fig. 3. (a,b,c,d): Wrapped images of the correlation fringes in the spectral field at wavelength 0.6328 μm for Zamzam water at different temperatures, 20°, 64°, 76°, and 80° respectively.

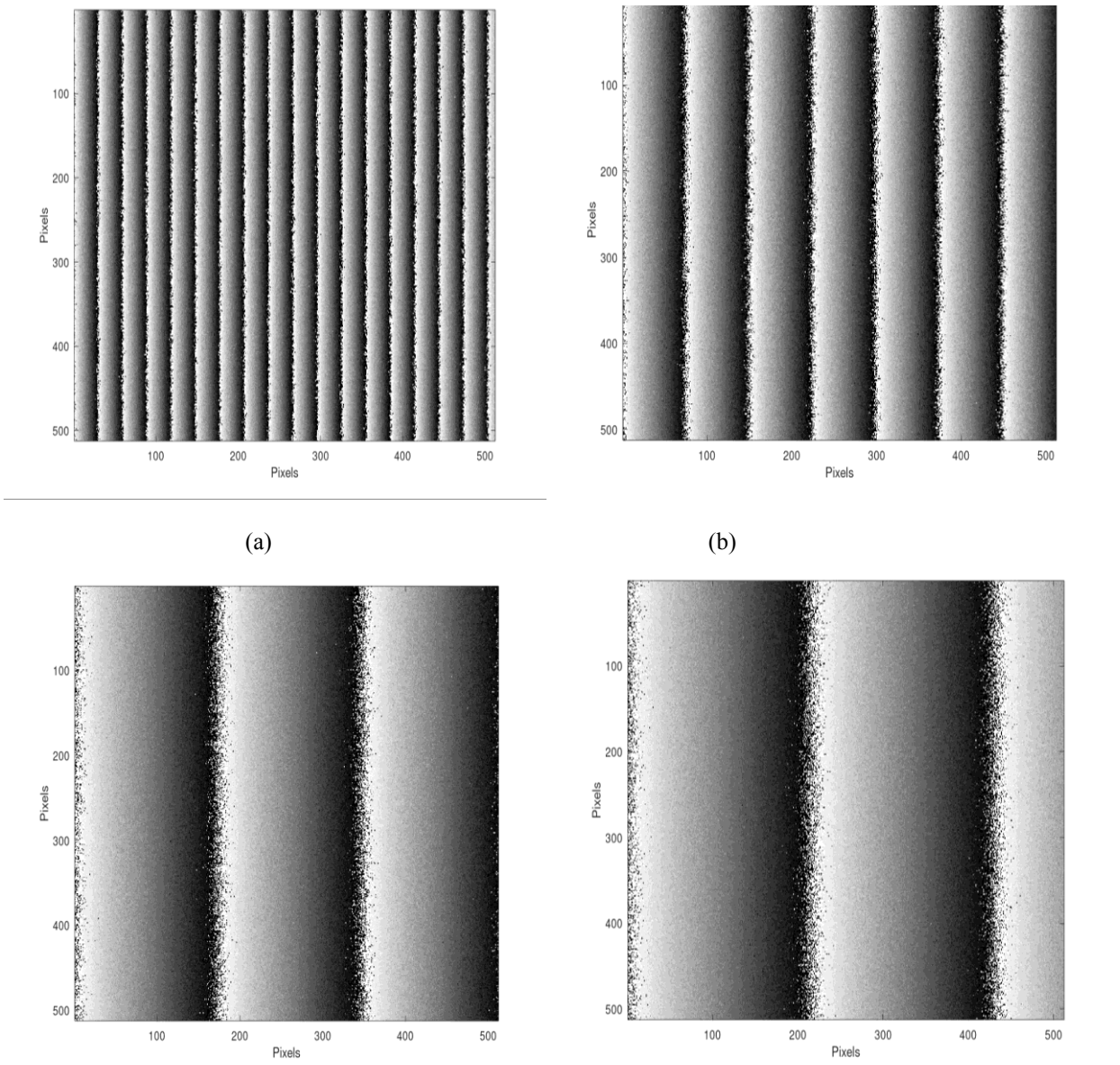

Fig. 4. (a,b,c,d): Wrapped images of the correlation fringes in the spectral field at wavelength 0.6328 μm for Bottled drinking water at different temperatures, 20°, 64°, 76°, and 80° respectively.

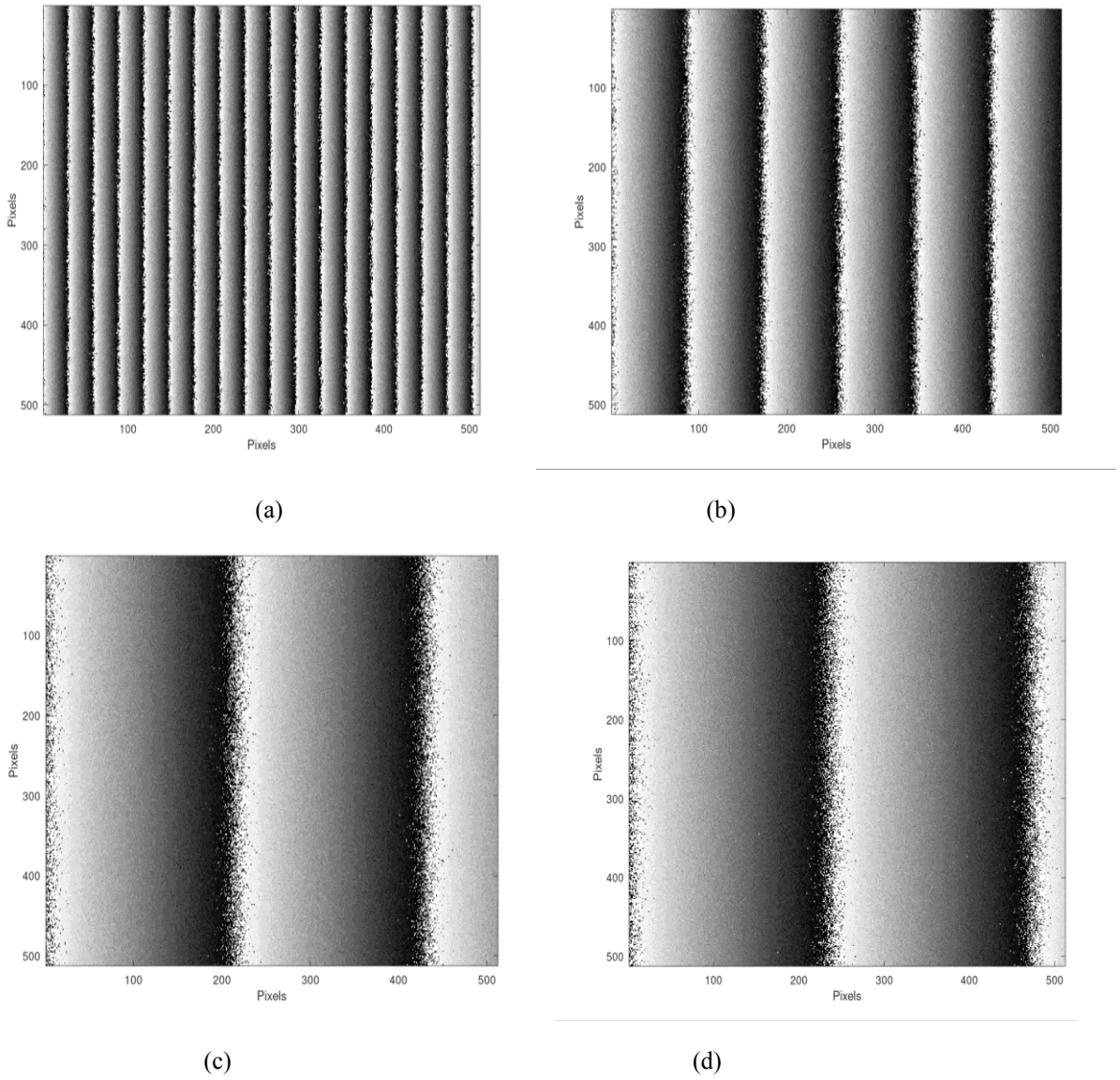

Fig. 5. (a,b,c,d): Wrapped images of the correlation fringes in the spectral field at wavelength 0.6328 μm for Distilled water at different temperatures, 20°, 64°, 76°, and 80° respectively.

Figures 6 (a,b,c,d), 7 (a,b,c,d), and 8 (a,b,c,d) show the wrapped images of the correlation fringes in the spectral field at wavelength 0.5461 μm for Zamzam, bottled drinking, and distilled waters at different temperatures, $20^{\circ}C$, $64^{\circ}C$, $76^{\circ}C$, and $80^{\circ}C$ respectively. The same phenomena can be observed as before. But in these figures, for Zamzam water, there are no wrapped images obtained due to the increasing temperature, as in the case at

$80^{\circ}C$. For bottled drinking water there are no wrapped images obtained at $80^{\circ}C$. For distilled water, the disappearing wrapped images at $76^{\circ}C$ and $80^{\circ}C$.

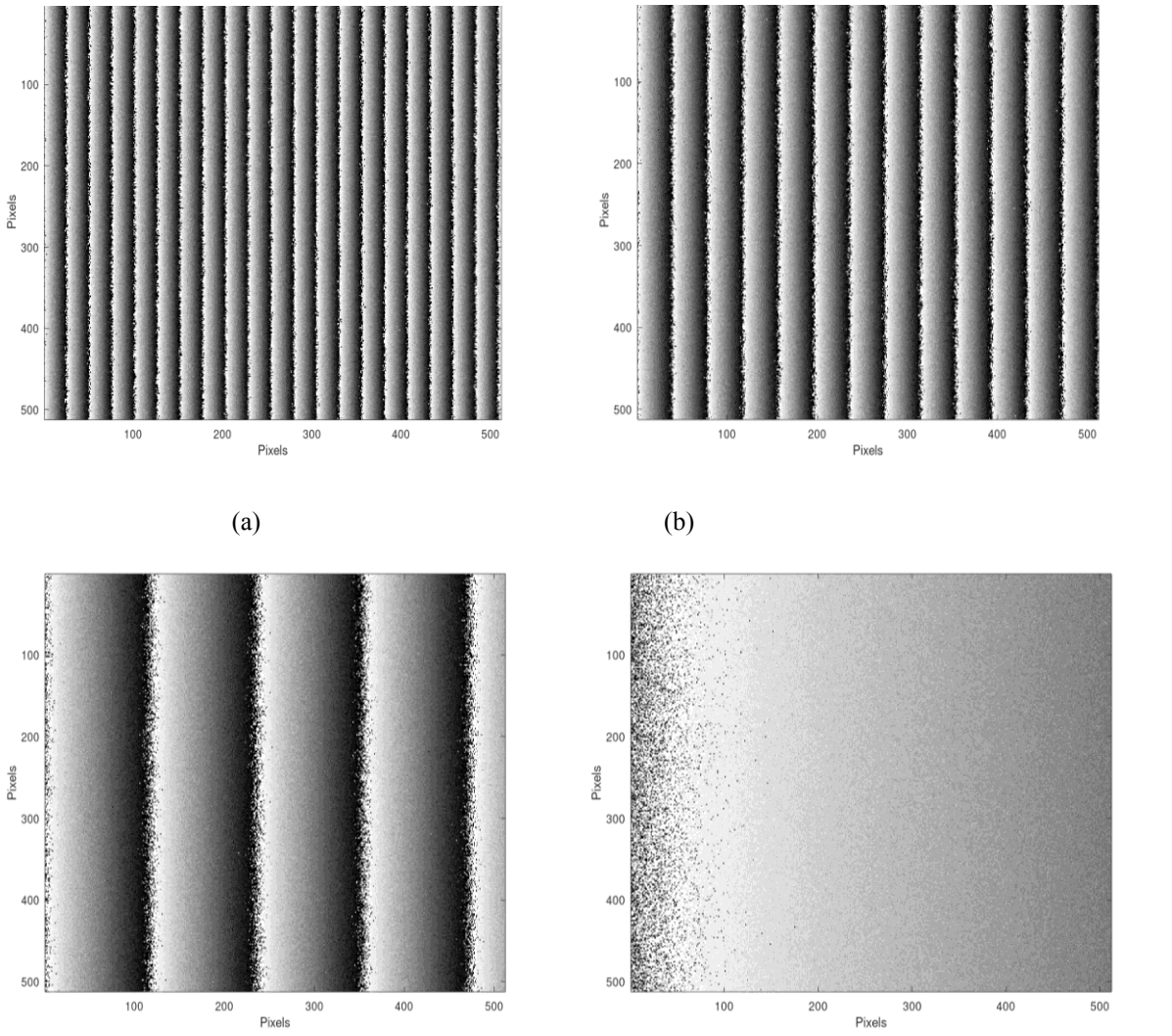

(a) (b)

(c) (d)

Fig. 6. (a,b,c,d): Wrapped images of the correlation fringes in the spectral field at wavelength 0.5461 μm for Zamzam water at different temperatures, 20°, 64°, 76°, and 80° respectively.

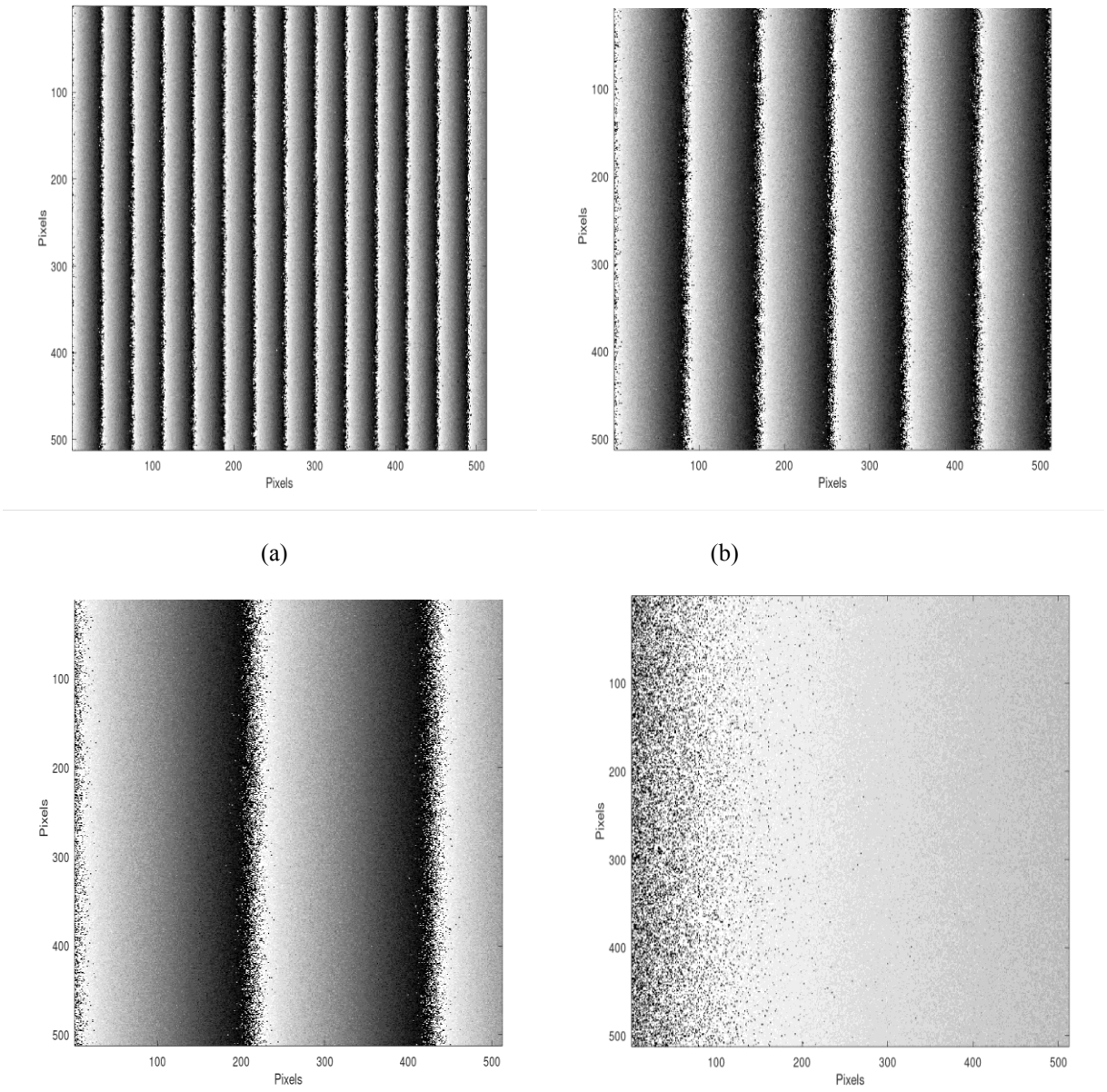

Fig. 7. (a,b,c,d): Wrapped images of the correlation fringes in the spectral field at wavelength 0.5461 μm for Bottled drinking water at different temperatures, 20°, 64°, 76°, and 80° respectively.

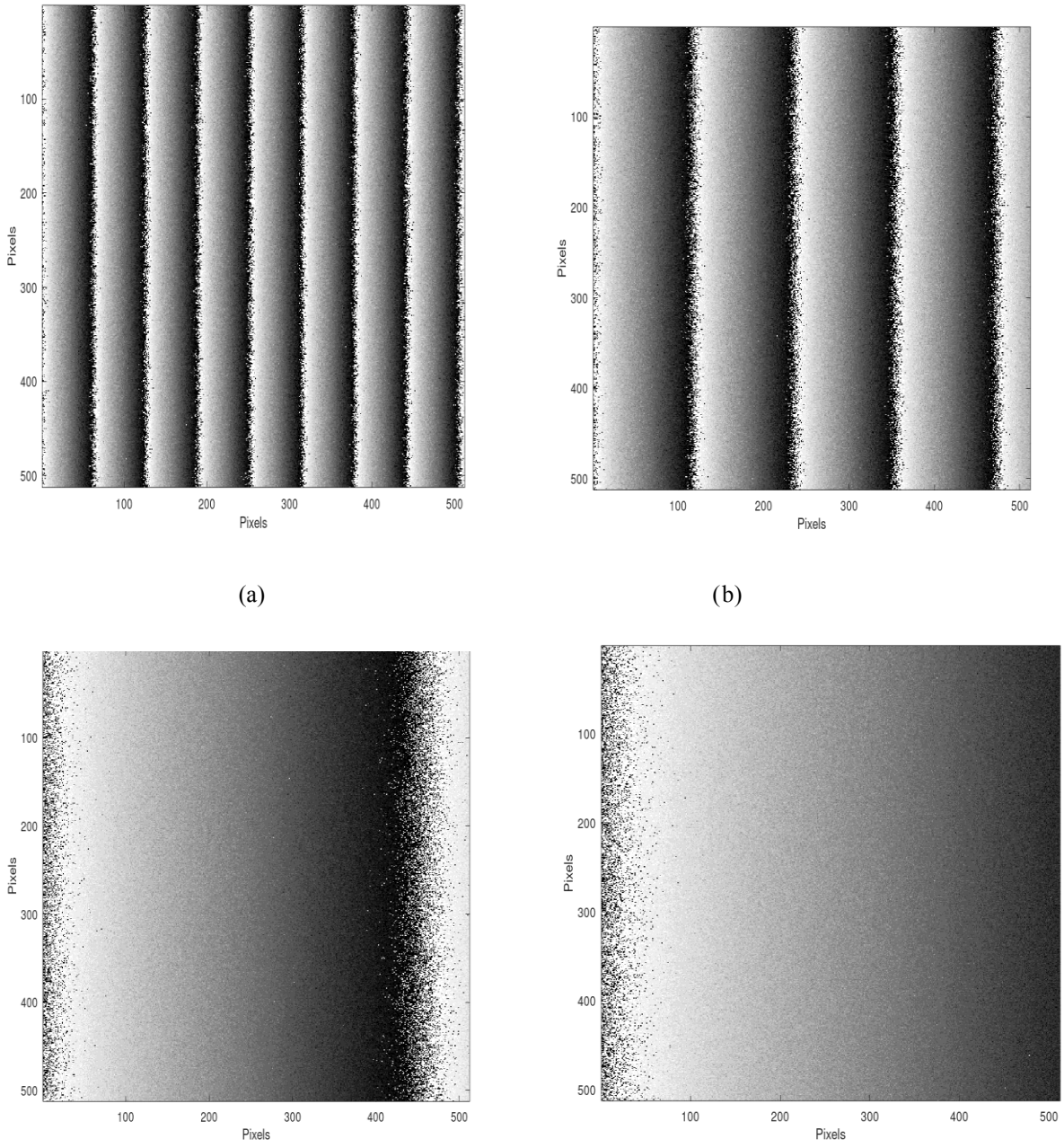

Fig. 8. (a,b,c,d): Wrapped images of the correlation fringes in the spectral field at wavelength 0.5461 μm for Distilled water at different temperatures, 20°, 64°, 76°, and 80° respectively.

Figures 9(a,b,c,d), 10(a,b,c,d) , and 11(a,b,c,d) show the wrapped images of the correlation fringes in the spectral field at wavelength 0.4047 μm for Zamzam, bottled drinking, and distilled waters at different temperatures, 20°, 64°, 76°, and 80° respectively.

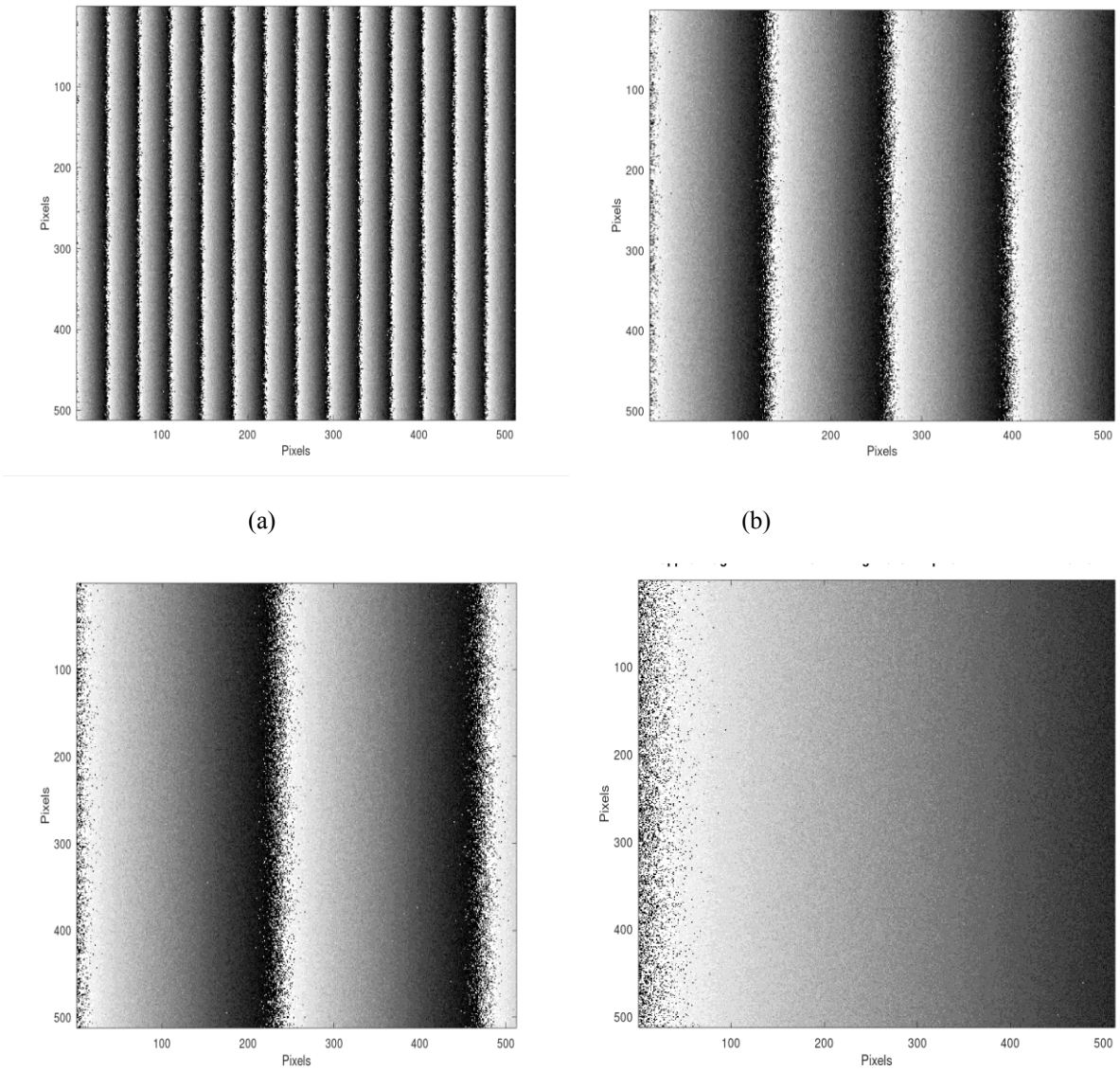

(a) (b)

(c) (d)

Fig. 9. (a,b,c,d): Wrapped images of the correlation fringes in the spectral field at wavelength 0.4047 μm for Zamzam water at different temperatures, 64°, 72°, 76°, and 80° respectively.

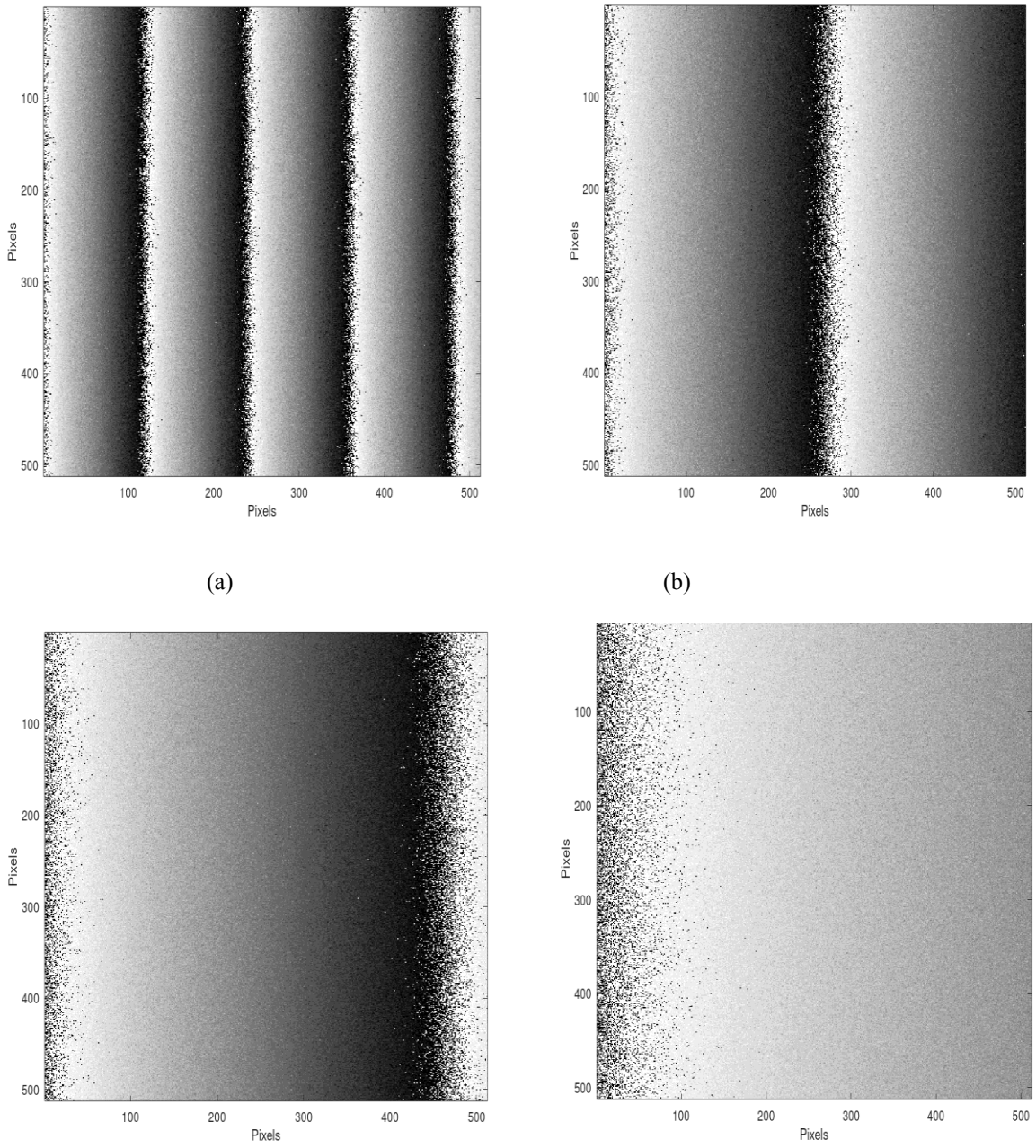

(a) (b)

(c) (d)

Fig. 10. (a,b,c,d): Wrapped images of the correlation fringes in the spectral field at wavelength 0.4047 μm for Bottled drinking water at different temperatures, $64^{\circ}, 72^{\circ}, 76^{\circ}$, and 80° respectively.

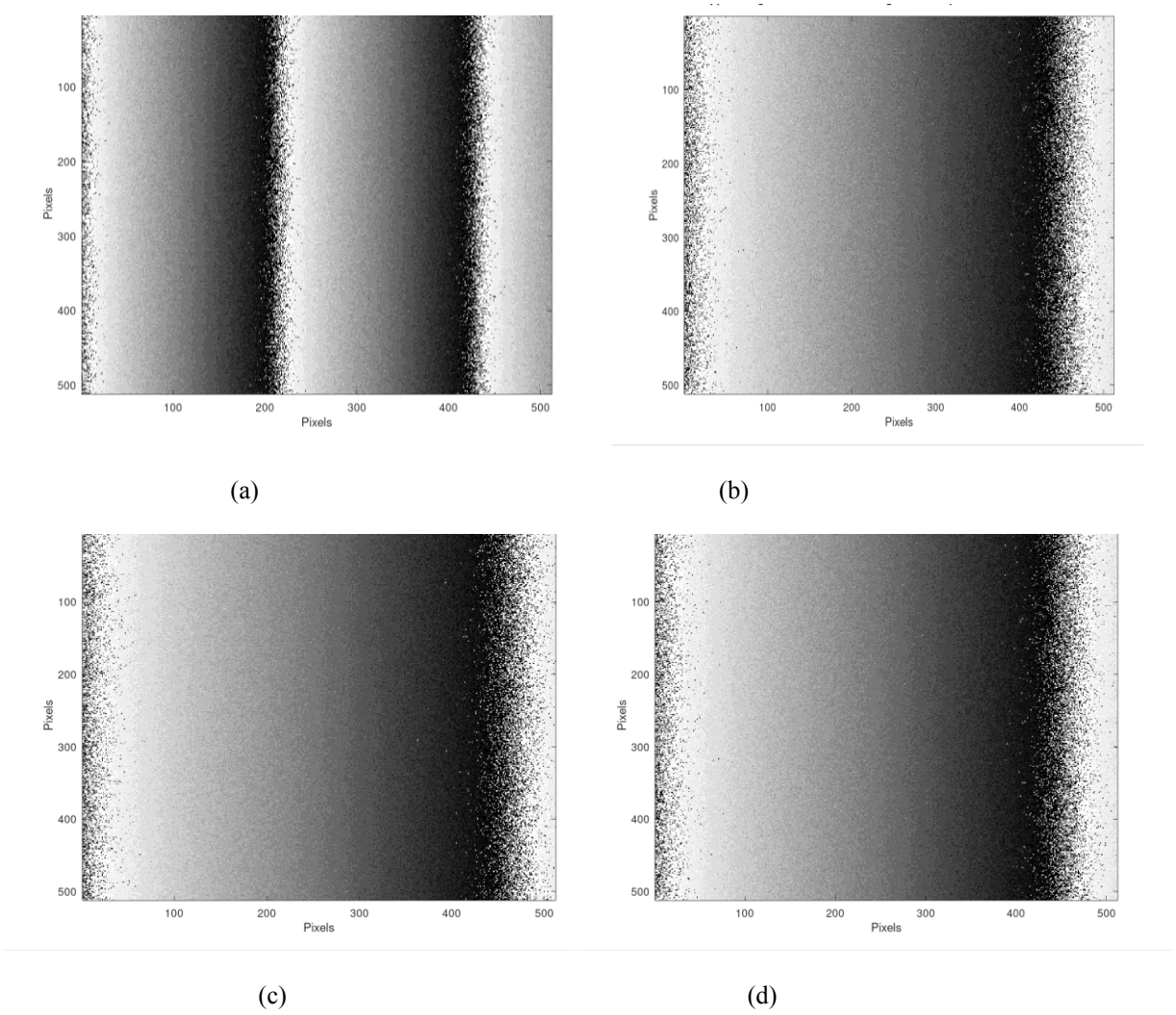

Fig. 11. (a,b,c,d): Wrapped images of the correlation fringes in the spectral field at wavelength 0.4047 μm for Distilled water at different temperatures, $64^{\circ}, 72^{\circ}, 76^{\circ}$, and 80° respectively.

As is obvious, for Zamzam water, there are no wrapped images obtained at $80^{\circ}C$. For bottled drinking water, there are no wrapped images obtained at $76^{\circ}C$ and $80^{\circ}C$. For distilled water, the disappearing wrapped images are at 72°, $76^{\circ}C$ and $80^{\circ}C$. From the previous figures, the wrapped images do not appear with increasing temperature, decreasing wavelength, or refractive index. This explains the superiority of appearing the wrapped images in the case of Zamzam water, even with high temperatures and low wavelengths, in comparison with the other mentioned waters.

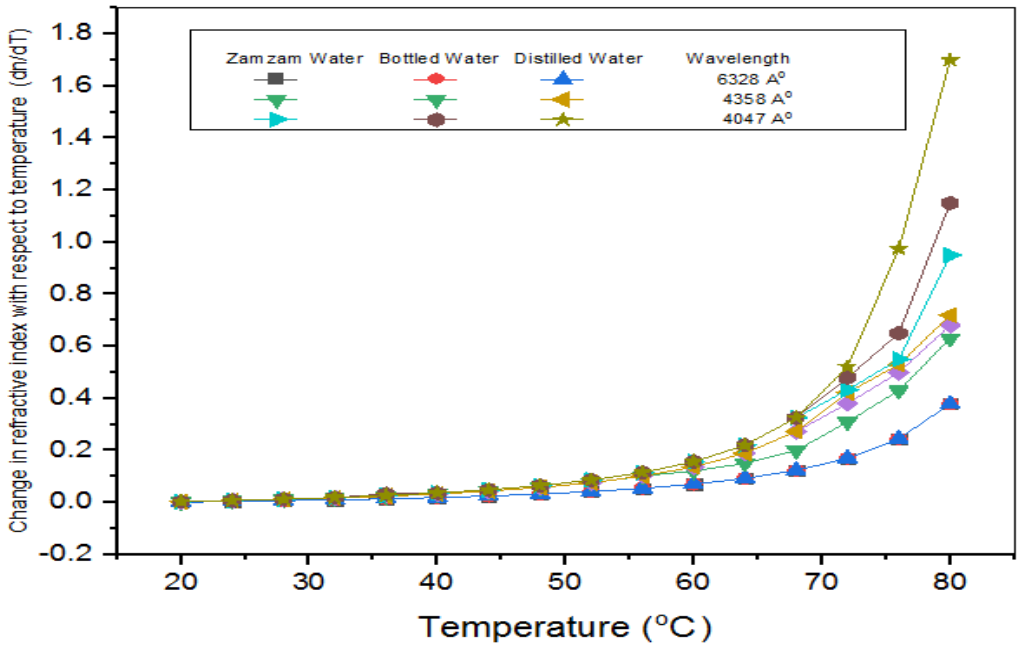

Fig. 12. Relation between the changes in refractive index due to the changes in temperature of the Zamzam, bottled drinking, and distilled waters at wavelengths of 0.6328 μm , 0.4358 μm , and 0.4047 μm , respectively.

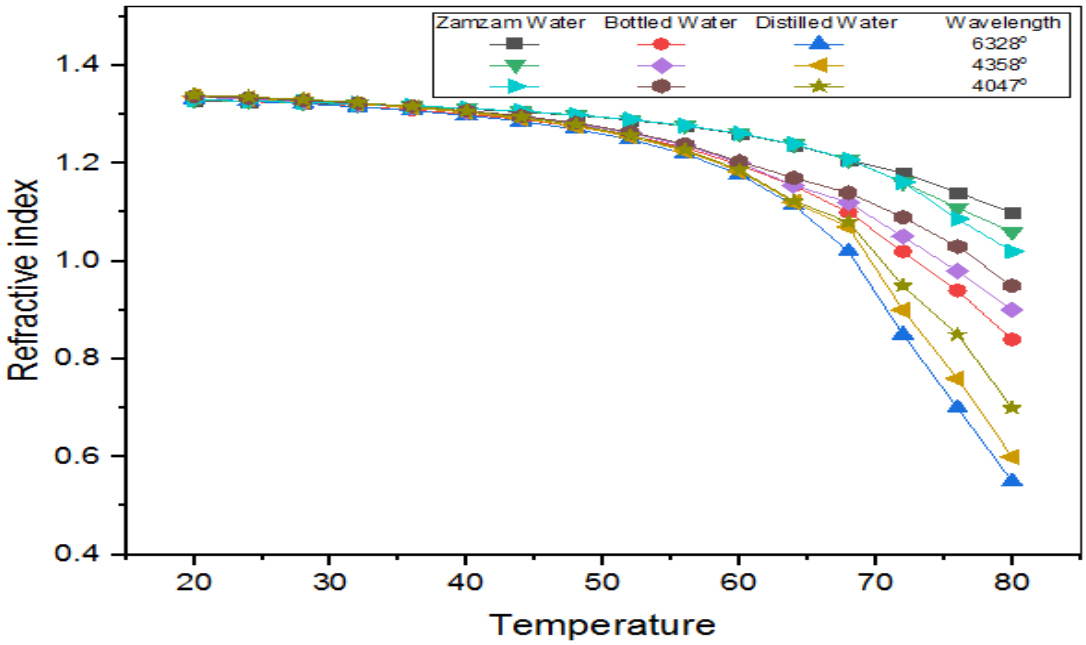

Fig. 13. Relation between the refractive index and temperature of Zamzam, bottled drinking, and distilled waters at wavelengths of 0.6328 μm , 0.4358 μm ,and 0.4047 μm respectively.

Figure (12) shows the relation between the changes in refractive index due to the changes in temperature of the Zamzam, bottled drinking, and distilled waters at wavelengths of 0.6328 μm, 0.4358 μm, and 0.4047 μm, respectively. As we can see, at the lowest temperatures from 20° to 32°, the changes in refractive index are very close in case of the different kinds of waters, although different wavelengths are used. At the highest temperatures and using different wavelengths, the changes in refractive index for the different waters diverge from each other. The changes in refractive index of Zamzam water are less affected by changes in temperature and wavelength, but in the case of distilled water, they are more affected.

Figure (13) shows the relation between the refractive index and temperature of Zamzam, bottled drinking, and distilled waters at wavelengths of 0.6328 μm, 0.4358 μm,and 0.4047 μm respectively. As we can see, at the temperatures ranges from 20° to $\approx 43^{\circ}$, the refractive index are very close in case of the different kinds of waters, although different wavelengths are used. At the highest temperatures and using different wavelengths, the refractive index for the different waters diverge from each other. The refractive index of Zamzam water are less affected by changes in temperature and wavelength, but in the case of distilled water, they are more affected.

Figure (14). Relation between the changes in refractive index with respect to wavelength and temperature of the Zamzam, bottled drinking water and distilled waters at wavelengths 0.6328 μm, 0.4358 μm,and 0.4047 μm respectively. As we can see, at the temperatures ranges from 20° to $\approx 33^{\circ}$, the change in refractive index with respect to wavelength $\frac{dn}{d\lambda}$ are very close in case of the different kinds of waters, although different wavelengths are used.

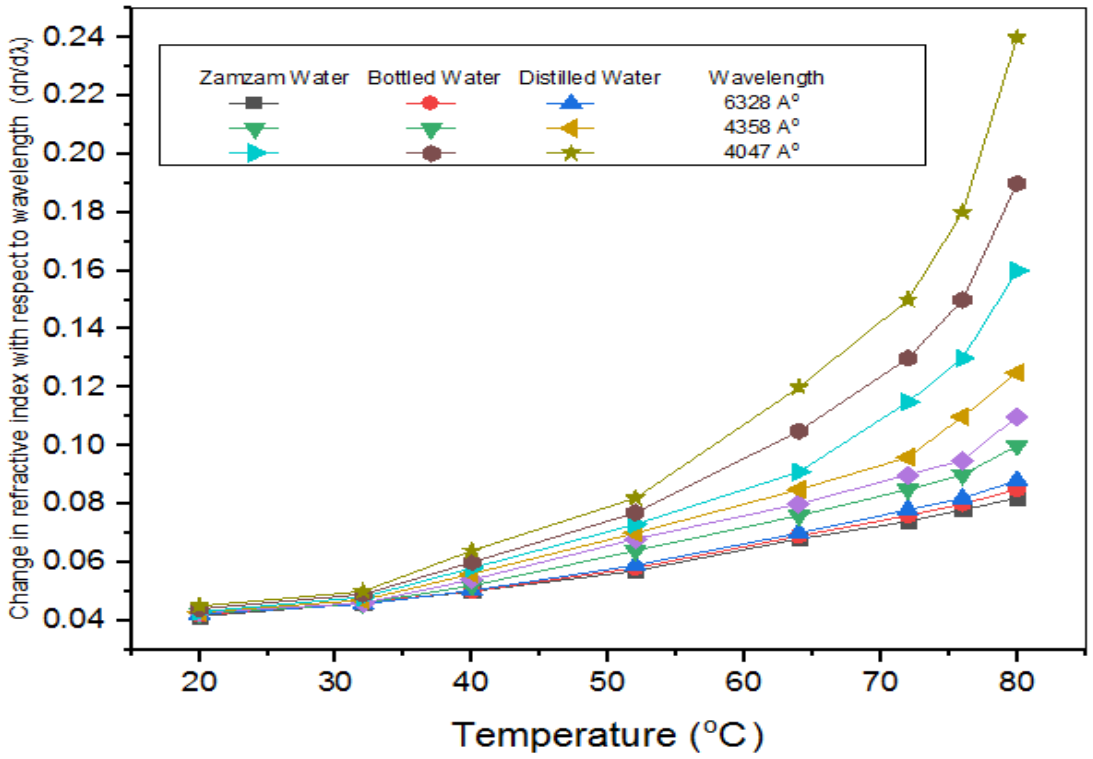

Fig. 14. Relation between the changes in refractive index with respect to wavelength and temperature of the Zamzam, bottled drinking water and distilled waters at wavelengths 0.6328 μm, 0.4358 μm ,and 0.4047 μm respectively.

At the highest temperatures, the change in refractive index with respect to wavelength $\frac{dn}{d\lambda}$ for the different waters diverge from each other. $\frac{dn}{d\lambda}$ of Zamzam water are less affected by changes in temperature and wavelength, but in the case of distilled water, they are more affected.

5. Conclusion

Variations of refractive indices of Zamzam, bottled drinking and distilled waters with wavelength and temperature in the range of 20^{o}C to 80^{o}C have been measured by computer simulation phase shifting digital interferometry at six discrete wavelengths across the visible spectrum. The dependence on temperature and wavelength were obtained. New theoretical model about the temperature and wavelength dependence of the refractive index of liquid is presented. A decrease of refractive index values with increasing temperature and an increase of change in refractive index with increasing temperature are observed. It can be concluded that the computer simulation measurements of the change in refractive is in good agreement with the theoretical new formulae, which also confirmed with the experimental results previously obtained. The superiority of appearing the wrapped images in case of Zamzam water even with high temperature and low wavelength in comparison with the other mentioned waters can be observed. Summary of saying that Zamzam water has special and distinguished optical refractive index that are different than those of bottled drinking and distilled waters.

References

1- Panta, G., & Subedi, D. (2013). Electrical characterization of aluminum (Al) thin films measured by using four- point probe method. *Kathmandu University Journal of Science, Engineering and Technology*, *8*(2), 31–36. https://doi.org/10.3126/kuset.v8i2.7322

2- Tan CY, Huang YX (2015) Dependence of Refractive Index on Concentration and Temperature in Electrolyte Solution, Polar Solution, Nonpolar Solution, and Protein Solution. J Chem Eng 60: 2827-2833. https://doi.org/10.1021/acs.jced.5b00018

3- W. Mahmood bin Mat Yunus and Azizan bin Abdul Rahman, "Refractive index of solutions at high concentrations," Appl. Opt. **27**, 3341-3343 (1988). https://opg.optica.org/ao/abstract.cfm?URI=ao-27-16-3341

4- Shao D, Tian L, Chen J, and Chen X (2010) Improved retroreflection method for measuring the refractive index of liquids. Appl Opt 49: 3049-3052. https://doi.org/10.1364/AO.49.003049

5- Grange BW, Stevenson WH, Viskanta R (1976) Refractive index of liquid solutions at low temperatures: an accurate measurement. Appl Opt 15: 858-859. https://doi.org/10.1364/AO.15.000858

6- Vilitis O, Shipkovs P, Merkulov D (2009) Determining the refractive index of liquids using a cylindrical cuvette. Meas Sci Technol 20**:** 117001.
https://**doi:** 10.1088/0957-0233/20/11/117001

7- Bashkatov AN, Genina EA (2003) Water refractive index in dependence on temperature and wavelength: a simple approximation. Proc. SPIE 5068, Saratov Fall Meeting 2002: Optical Technologies in Biophysics and Medicine IV. http://doi.org/10.1117/12.518857

8- Jenkins, D.D. (1982) Refractive Indices of Solutions. Physics Education, 17, 82. https://doi.org/10.1088/0031-9120/17/2/413

9- Boulay, R., Gagnon, R., Rochette, D., et al. (1984) Paper Sheet Moisture Measurements in the Far Infrared. International Journal of Infrared and Millimeter Waves, 5, 1221-1234. https:// doi.org/10.1007/BF01010048

10- Bass, J.D. and Weidner, D.J. (1984) Method for Measuring the Refractive Index of Transparent Solids. Review of Scientific Instruments, 55, 1569.
https:// doi.org/10.1063/1.1137611

11- Nasser A. Moustafa, Hasan Assaedi, and Thamer H. Albaqami (2023) Accurate computer simulation phase-shifting digital interferometry for measurement of the optical properties of Zamzam water in the visible spectrum. Egyptian journal of physics. *Egypt. J. Phys.* Vol. 51, pp. 165-185 (2023): doi:10.21608/EJPHYSICS.2023.225657.1090

12- Nasser A. Moustafa, "Digital Processing of Speckle Photography to Measure Refractive Index of a Transparent Plate, Australian Journal of Basic and Applied Sciences, 7(8), 187 -193, 2013. http://doi:10.1117/12.2020374

13- Nasser A. Moustafa, Hasan Assaedi, and Thamer H. Albaqami "Comparative study of Zamzam, bottled drinking and distilled waters by a novel computer simulation speckle photography method using Fourier transform", Open Journal of Applied Sciences,12, 1577-1594 (2022). https://doi.org/10.4236/ojapps.2022.129107

14- Nasser A.Moustafa, "Active Speckle Photography Method Using Fourier Transform for Measuring the Thickness of A Transparent Plate, " International Journal of Physics and Research (IJPR), Vol. 3, Issue 3, 61-72, 2013. Academia.edu/4132538

15- Nasser A. Moustafa, "Comparative measurement in speckle interferometry interferometry using holographically generated reference wave using the single reference beam technique", Opt. Commun. 172 (1-6) (1999) 9-16.

http://doi:10.1016/S0030-4018(99)00415-0

16- Hongchun Gao, Yi Jiang, Liuchao Zhang, Lan Jiang, "Five-step phase-shifting white-light interferometry for the measurement of fiber optic extrinsic Fabry-Perot interferometers", Appl Opt. 2018 Feb 10;57(5):1168-1173.

http://doi: 10.1364/AO.57.001168

17- Nasser A. Moustafa, Hasan Assaedi, and Thamer H. Albaqami, "Comparative study of Zamzam, bottled drinking and distilled waters by a novel computer simulation speckle photography method using Fourier transform", Open Journal of Applied Sciences,12, 1577-1594 (2022). https://doi.org/10.4236/ojapps.2022.129107